Supplementary Information for

Large potential for crop production adaptation depends on available future varieties

Florian Zabel, Christoph Müller, Joshua Elliott, Sara Minoli, Jonas Jägermeyr, Julia M. Schneider, James A. Franke, Elisabeth Moyer, Marie Dury, Louis Francois, Christian Folberth, Wenfeng Liu, Thomas A. M. Pugh, Stefan Olin, Sam S. Rabin, Wolfram Mauser, Tobias Hank, Alex C. Ruane, Senthold Asseng

Correspondence to: f.zabel@lmu.de

This PDF file includes:

- Table S1
- Figs. S1 to S20
- Supplementary Note 1 & 2

Table S1: Participating crop models with main references.

GGCM	Simulated Crops	References
CARAIB	Maize, Soy, Rice, Winter wheat, Spring wheat	(*1, 2*)
GEPIC	Maize, Soy, Rice, Winter wheat, Spring wheat	(*3, 4*)
LPJ-GUESS	Maize, Winter wheat, Spring wheat	(*5, 6*)
LPJmL	Maize, Soy, Rice, Winter wheat, Spring wheat	(*7*)
pDSSAT	Maize, Soy, Rice, Winter wheat, Spring wheat	(*8, 9*)
PEPIC	Maize, Soy, Rice, Winter wheat, Spring wheat	(*10, 11*)
PROMET	Maize, Soy, Rice, Winter wheat, Spring wheat	(*12-14*)

References:

1. M. Dury et al., Responses of European forest ecosystems to 21st century climate: Assessing changes in interannual variability and fire intensity. iForest : Biogeosciences and Forestry 4, (2011).
2. N. Pirttioja et al., Temperature and precipitation effects on wheat yield across a European transect: A crop model ensemble analysis using impact response surfaces. Climate Research 65, 87-105 (2015).
3. J. Liu, J. Williams, A. Zehnder, H. Yang, GEPIC— Modelling Wheat Yield and Crop Water Productivity with High Resolution on a Global Scale. Agricultural Systems 94, 478-493 (2007).
4. C. Folberth, T. Gaiser, K. C. Abbaspour, R. Schulin, H. Yang, Regionalization of a large-scale crop growth model for sub-Saharan Africa: Model setup, evaluation, and estimation of maize yields. Agriculture, Ecosystems & Environment 151, 21-33 (2012).
5. M. Lindeskog et al., Implications of accounting for land use in simulations of ecosystem carbon cycling in Africa. Earth Syst. Dynam. 4, 385-407 (2013).
6. S. Olin et al., Modelling the response of yields and tissue C : N to changes in atmospheric CO_2 and N management in the main wheat regions of western Europe. Biogeosciences 12, 2489-2515 (2015).
7. W. von Bloh et al., Implementing the nitrogen cycle into the dynamic global vegetation, hydrology, and crop growth model LPJmL (version 5.0). Geosci. Model Dev. 11, 2789-2812 (2018).
8. J. Elliott et al., The parallel system for integrating impact models and sectors (pSIMS). Environmental Modelling & Software 62, 509-516 (2014).
9. J. W. Jones et al., The DSSAT cropping system model. European Journal of Agronomy 18, 235-265 (2003).
10. W. Liu et al., Global investigation of impacts of PET methods on simulating crop-water relations for maize. Agr Forest Meteorol 221, 164-175 (2016).
11. W. Liu et al., Global assessment of nitrogen losses and trade-offs with yields from major crop cultivations. Science of the Total Environment 572, 526-537 (2016).
12. W. Mauser et al., Global biomass production potentials exceed expected future demand without the need for cropland expansion. Nat Commun 6 (2015).
13. F. Zabel et al., Global impacts of future cropland expansion and intensification on agricultural markets and biodiversity. Nature Communications 10, 2844 (2019).
14. T. B. Hank, H. Bach, W. Mauser, Using a Remote Sensing-Supported Hydro-Agroecological Model for Field-Scale Simulation of Heterogeneous Crop Growth and Yield: Application for Wheat in Central Europe. Remote Sensing 7, 3934-3965 (2015).

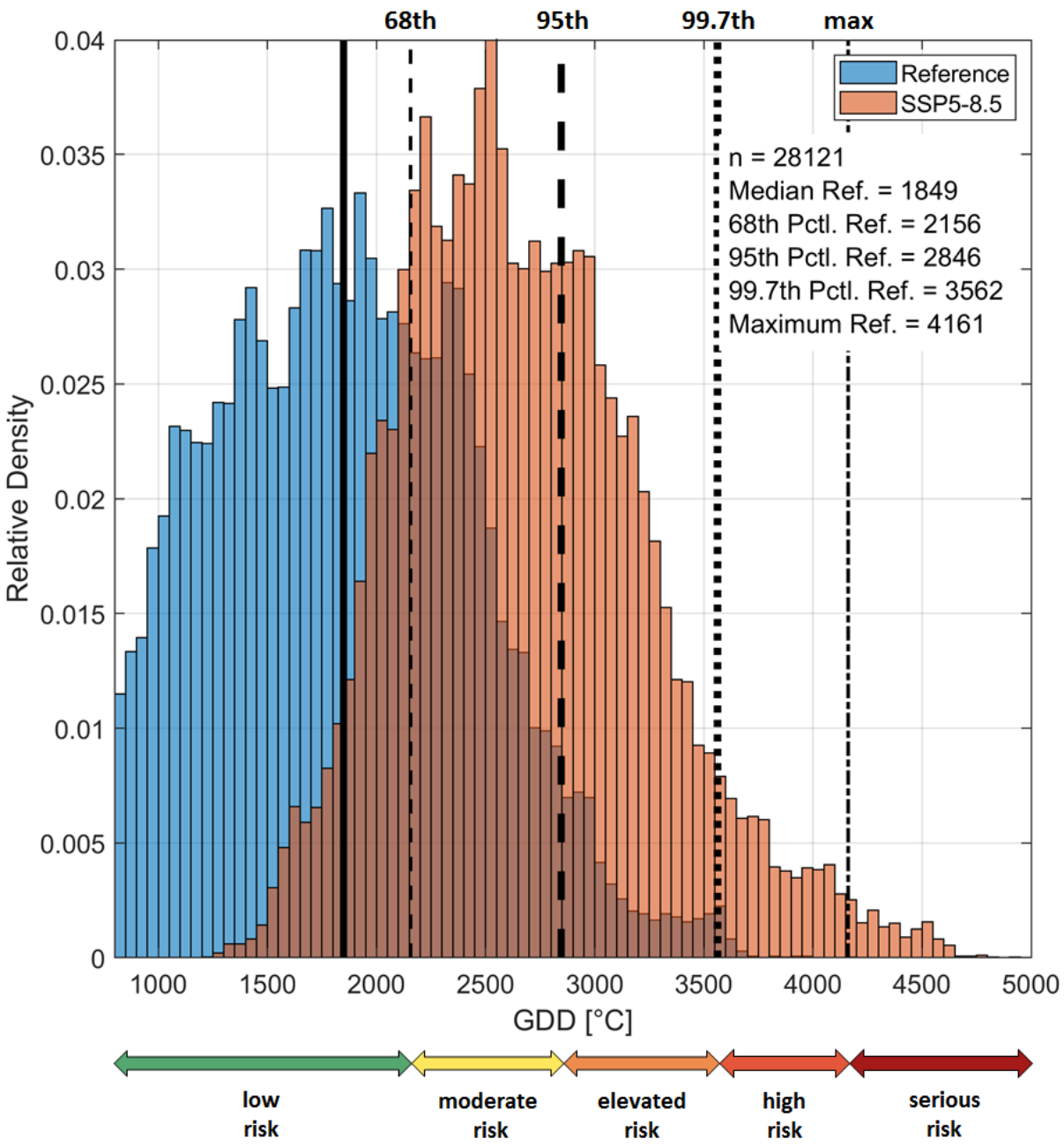

Figure S1: Histogram of globally distributed GDDs for maize, exemplarily for the climate model IPSL-CM6A-LR for SSP5-8.5. Blue bars show the distribution of GDD_{ref} for the reference climate period (1980-2010), while red bars show the distribution of GDD_{fut} for SSP5-8.5 (2070-2100). GDD values that are below a threshold required for flowering are not considered. The bold black line shows the median of GDD_{ref}, the dashed black lines show the 68th and 95th percentile and the maximum data of GDD_{ref}. The number of samples (n), and values for medians and 95th percentiles are given in the plot. The classification of risk classes (low risk, moderate risk, elevated risk, and serious risk) according to the percentile distribution is shown below the plot.

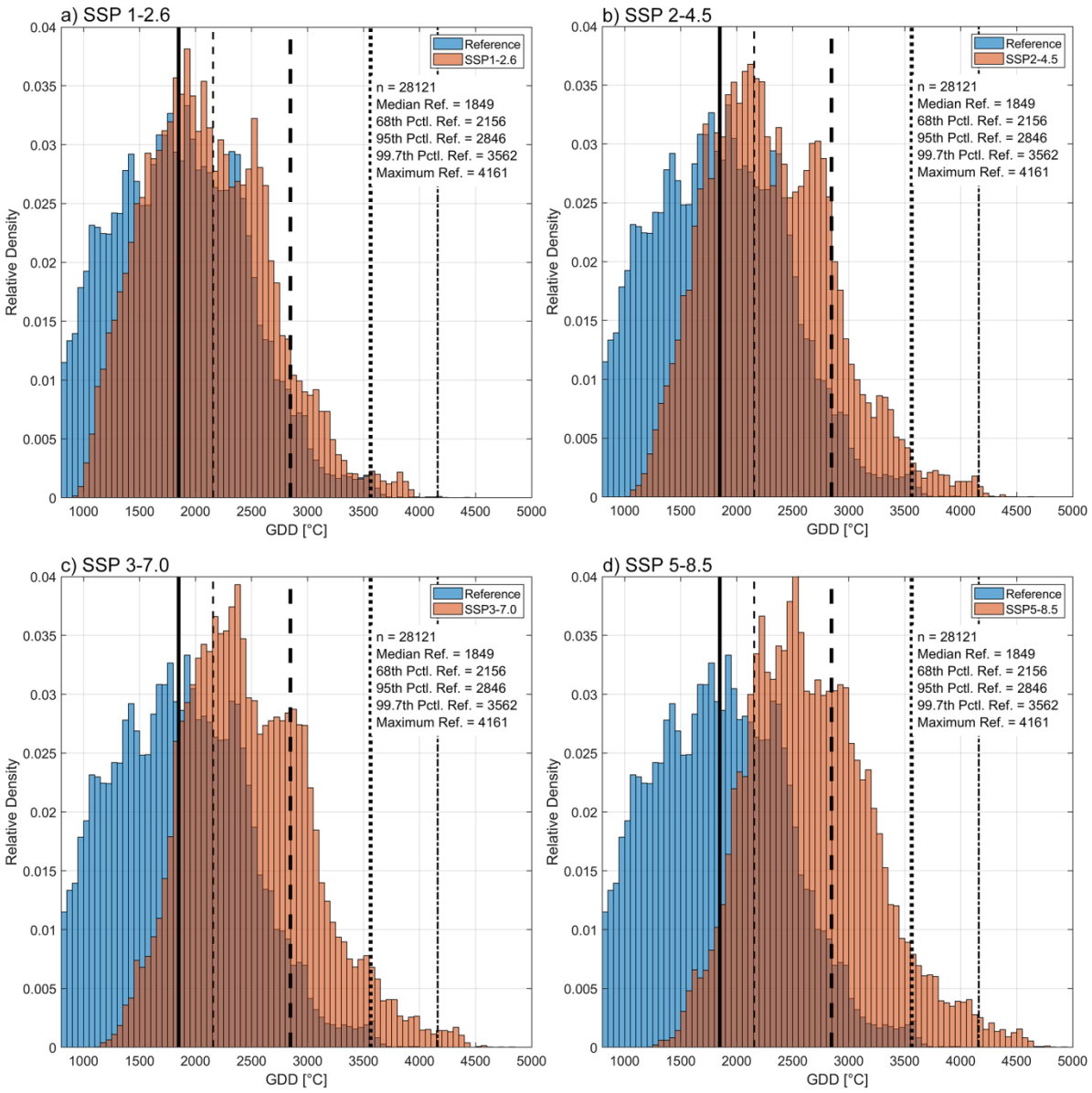

Figure S2: Histogram of globally distributed GDDs for maize, exemplarily for the climate model IPSL-CM6A-LR for SSPs 1-2.6 (a), 2-4.5 (b), 3-7.0 (c) and 5-8.5 (d). Blue bars show the distribution of GDD_{ref} for the reference climate period (1980-2010), while red bars show the distribution of GDD_{fut} for the respective SSP (2070-2100). GDD values that are below a threshold required for flowering are not considered. The bold black line shows the median of GDD_{ref}, the dashed black lines show the 68^{th} and 95^{th} percentile and the maximum data of GDD_{ref}. The number of samples (n), and values for medians and 95th percentiles are given in the plot.

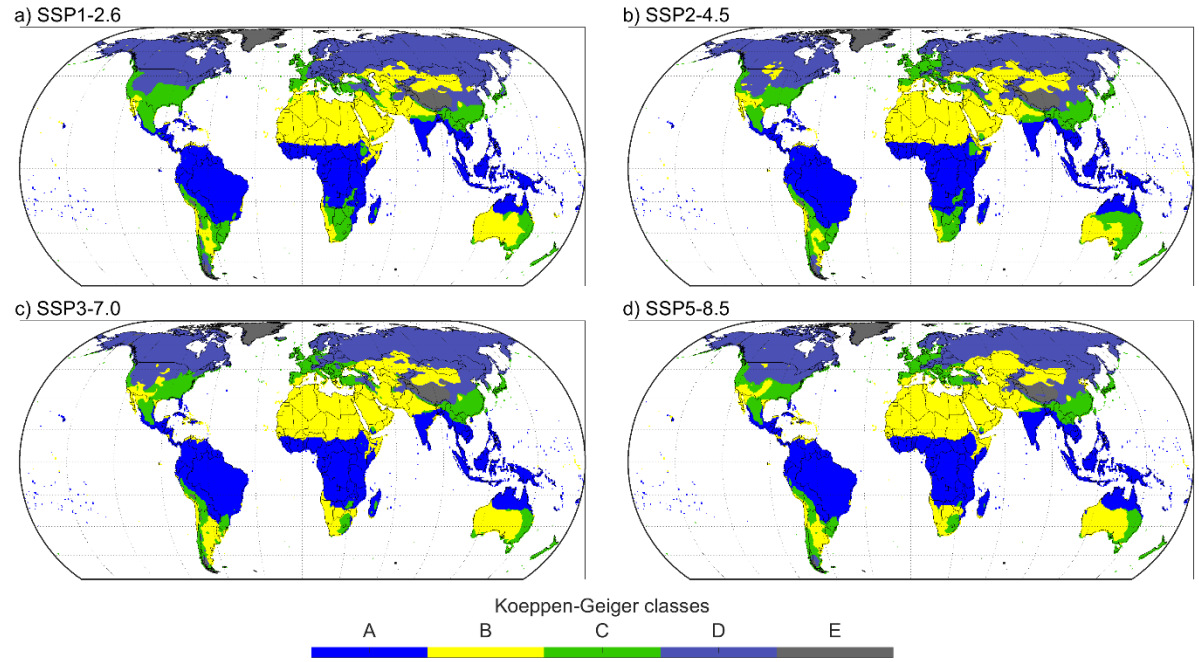

Figure S3: Koeppen-Geiger zones exemplarily for IPSL-CM6A-LR for SSPs 1-2.6 (a), 2-4.5 (b), 3-7.0 (c) and 5-8.5 (d). Class A: tropical, B: arid, C: temperate, D: cold, E: polar.

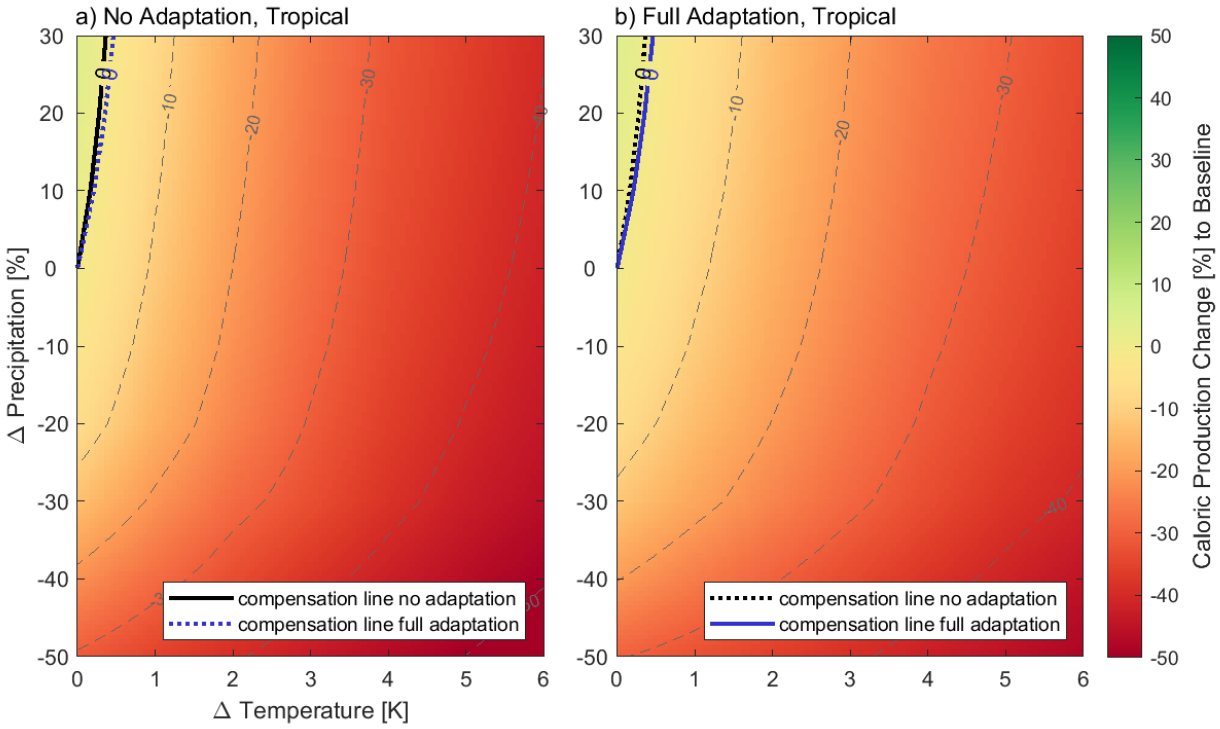

Figure S4: Response surfaces (a) without and (b) with full variety adaptation showing median values for the Koeppen-Geiger region A (tropical).

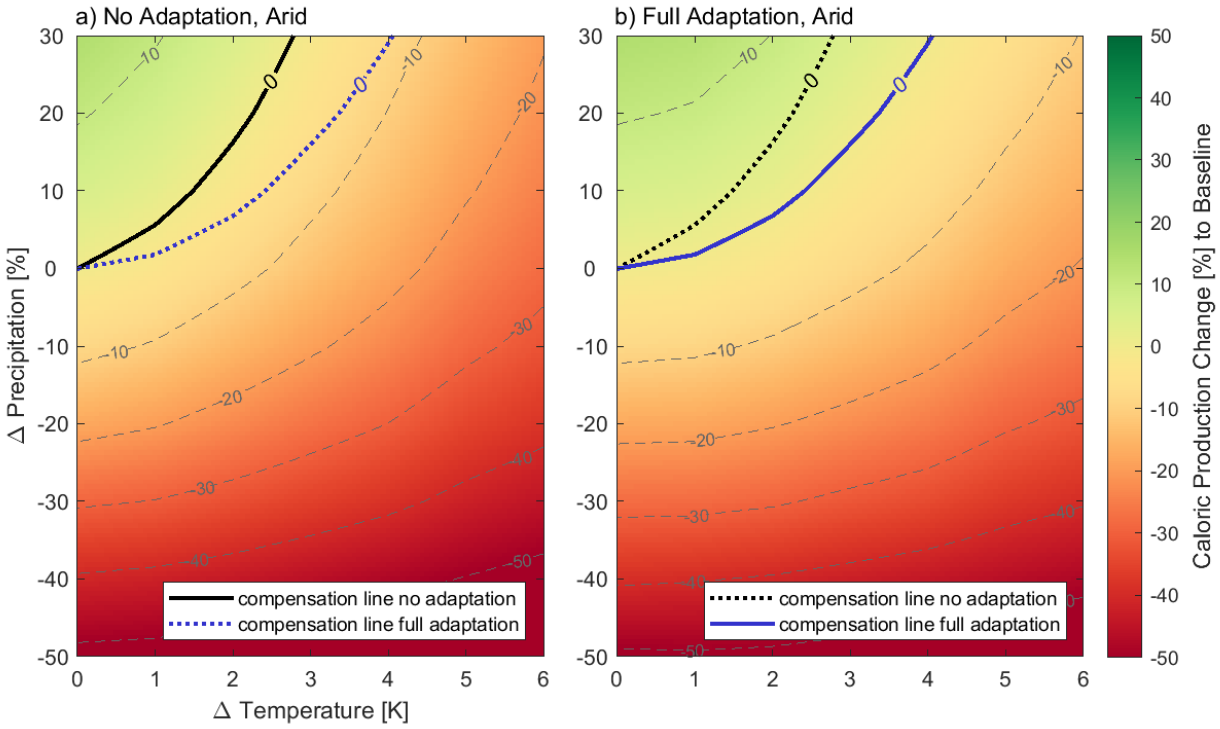

Figure S5: Response surfaces (a) without and (b) with full variety adaptation showing median values for the Koeppen-Geiger region B (arid).

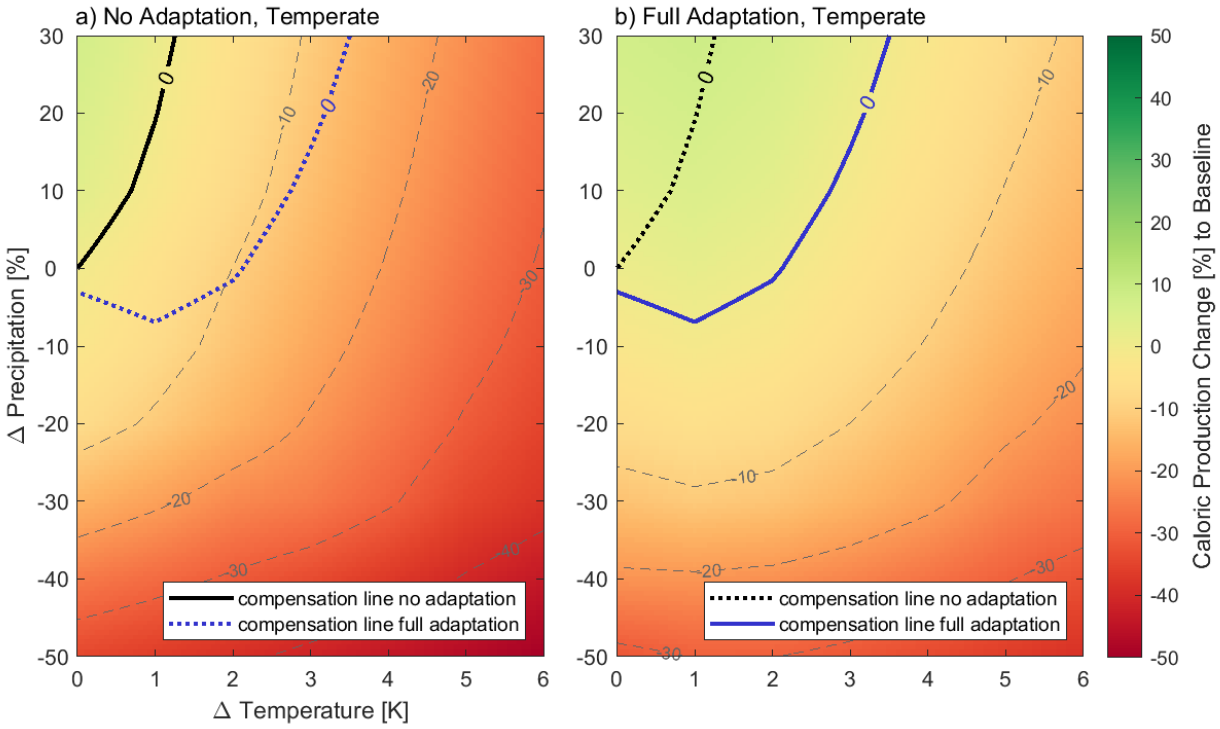

80

Figure S6: Response surfaces (a) without and (b) with full variety adaptation showing median values for the Koeppen-Geiger region C (temperate).

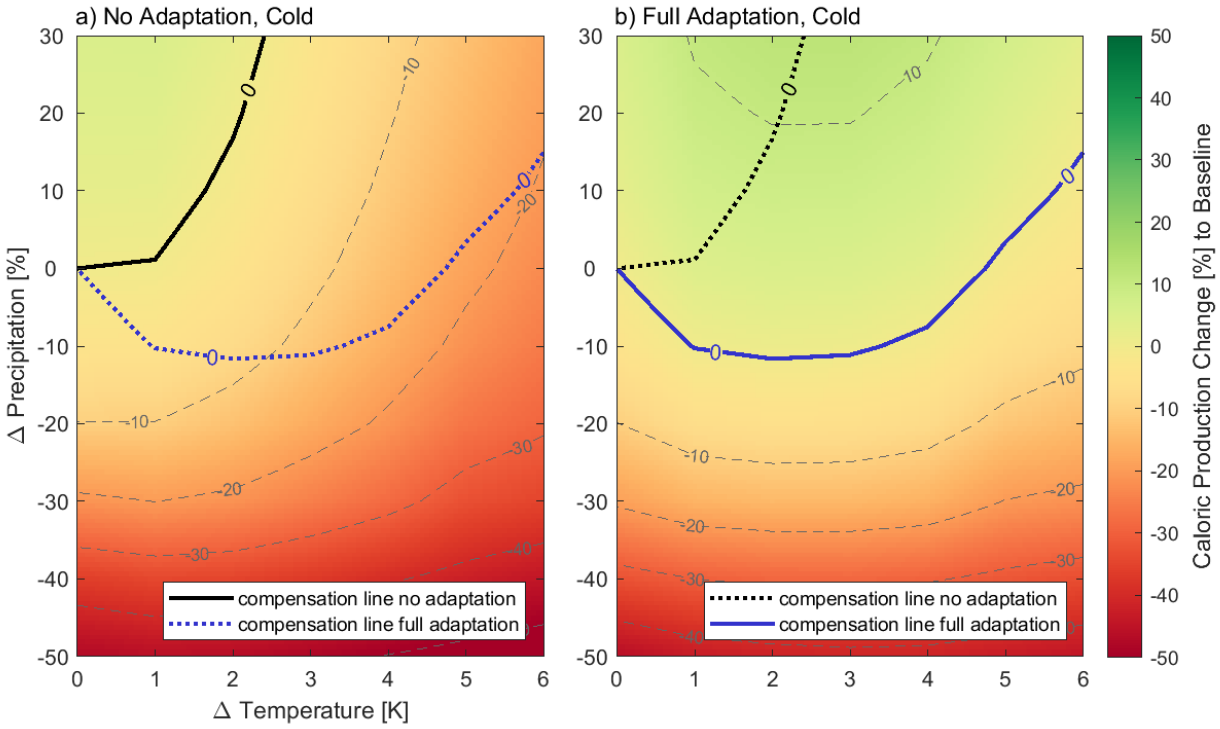

Figure S7: Response surfaces (a) without and (b) with full variety adaptation showing median values for the Koeppen-Geiger region D (cold).

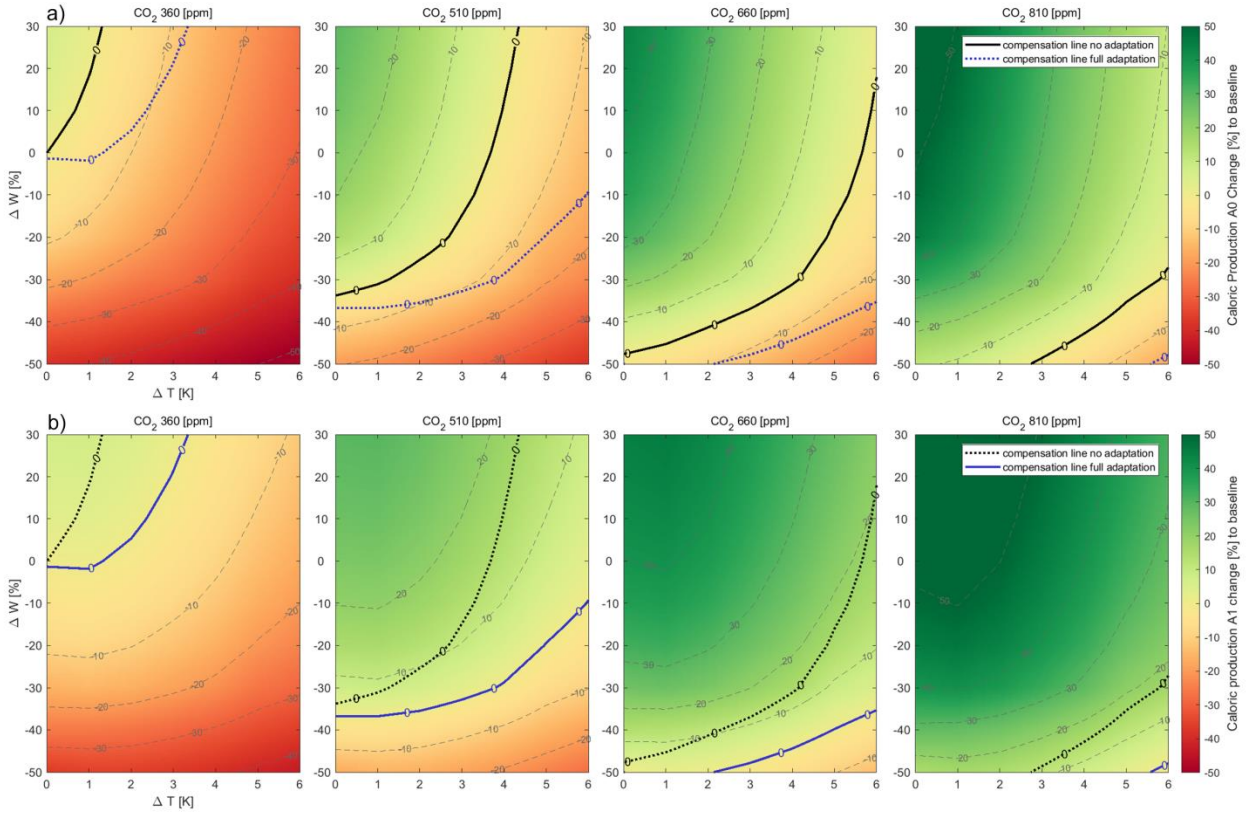

Figure S8: Response surfaces (a) without and (b) with full variety adaptation for four different CO_2 concentration levels, showing global median values.

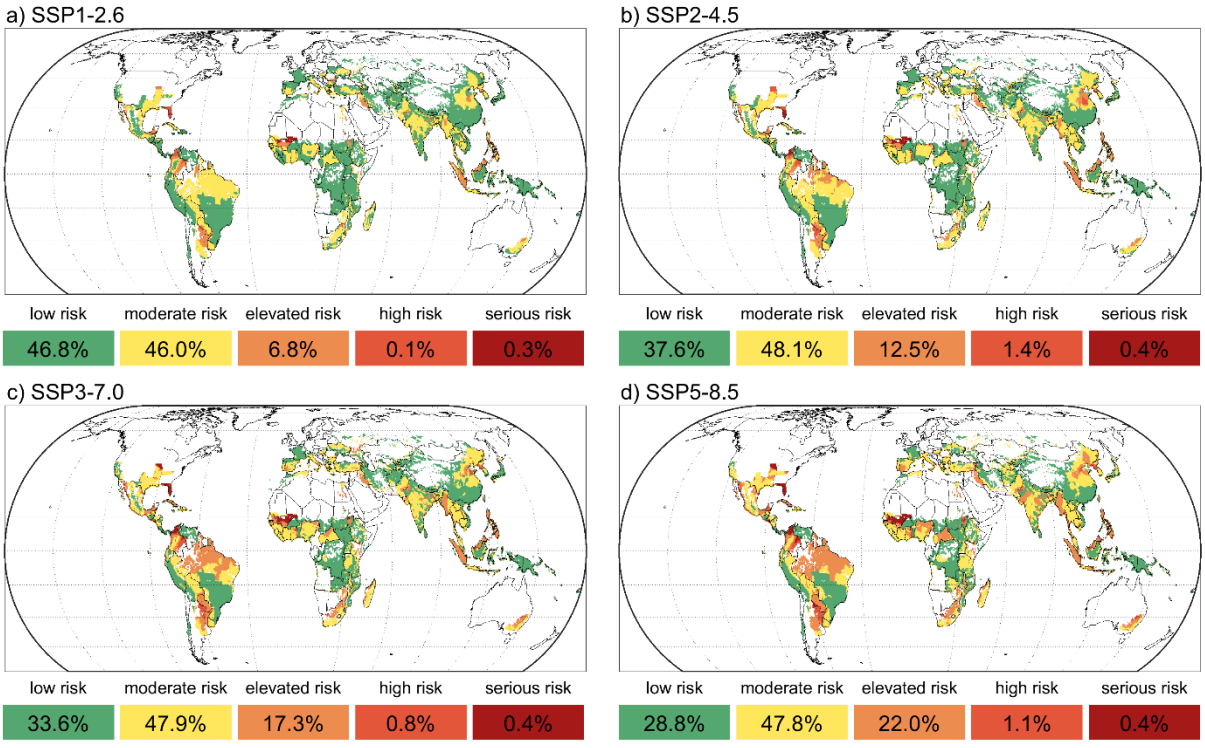

Figure S9: Same as Figure 4, but for rice.

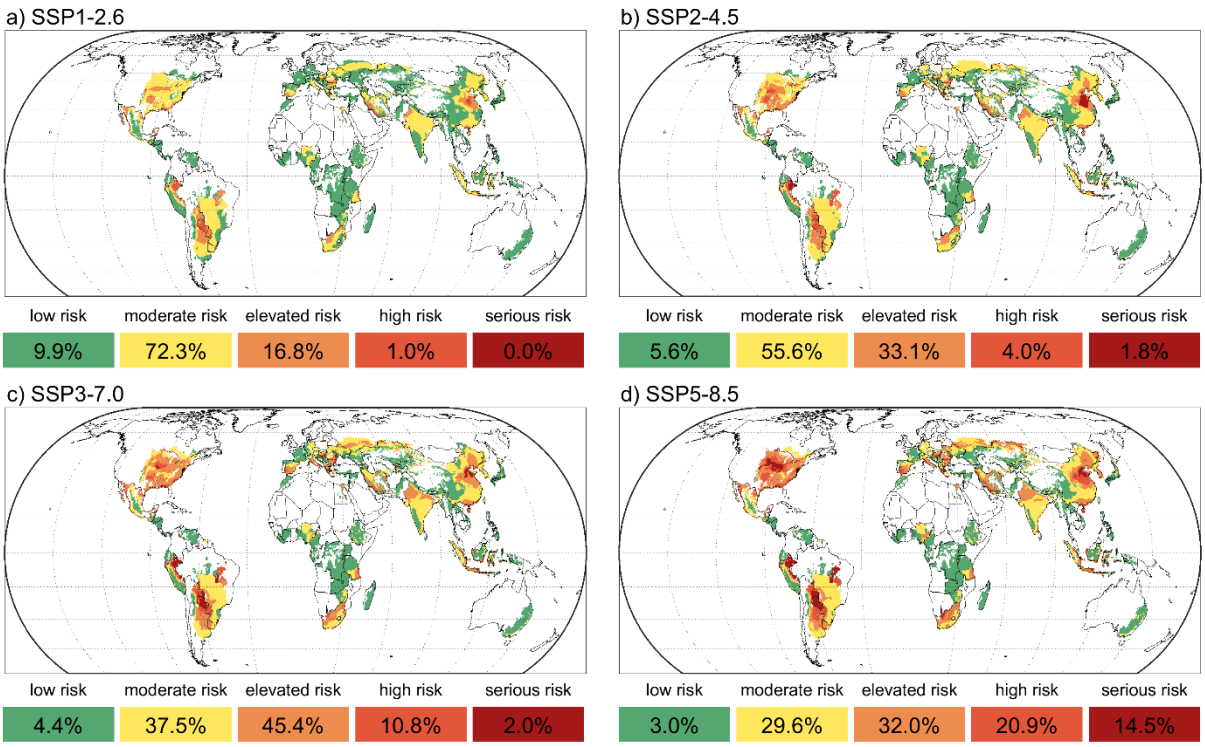

Figure S10: Same as Figure 4, but for soy.

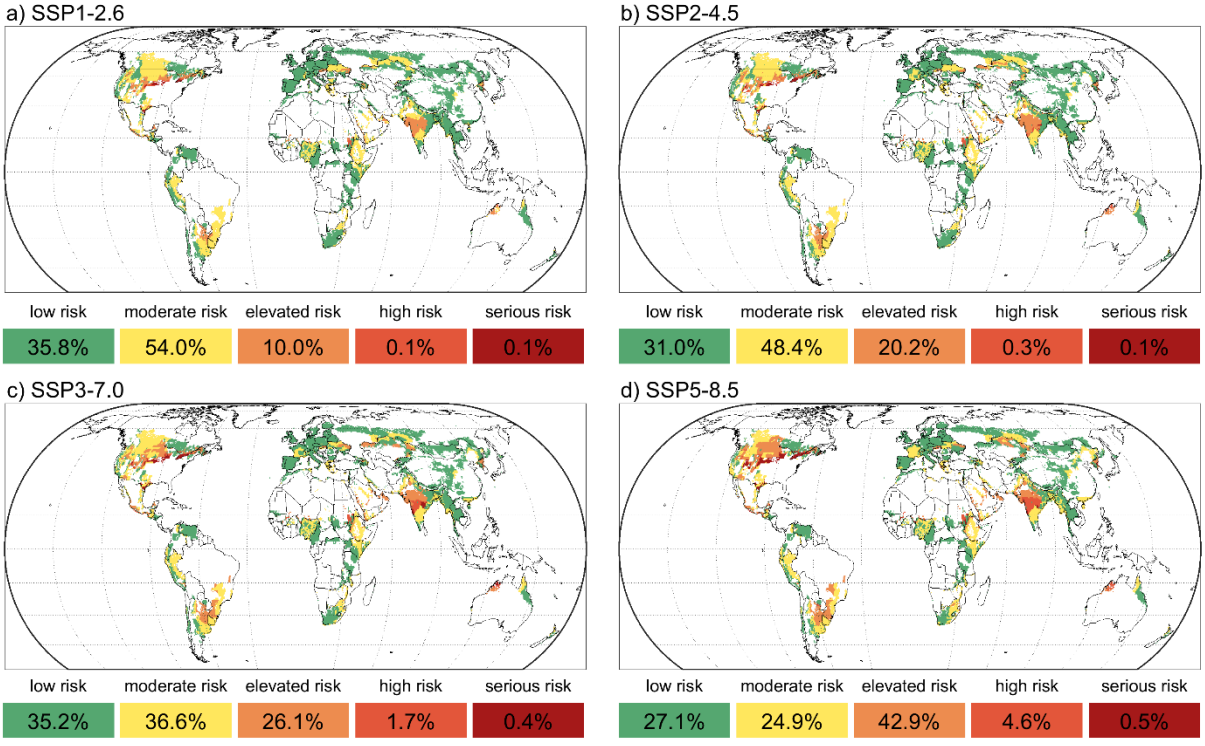

95 **Figure S11:** Same as Figure 4, but for spring wheat.

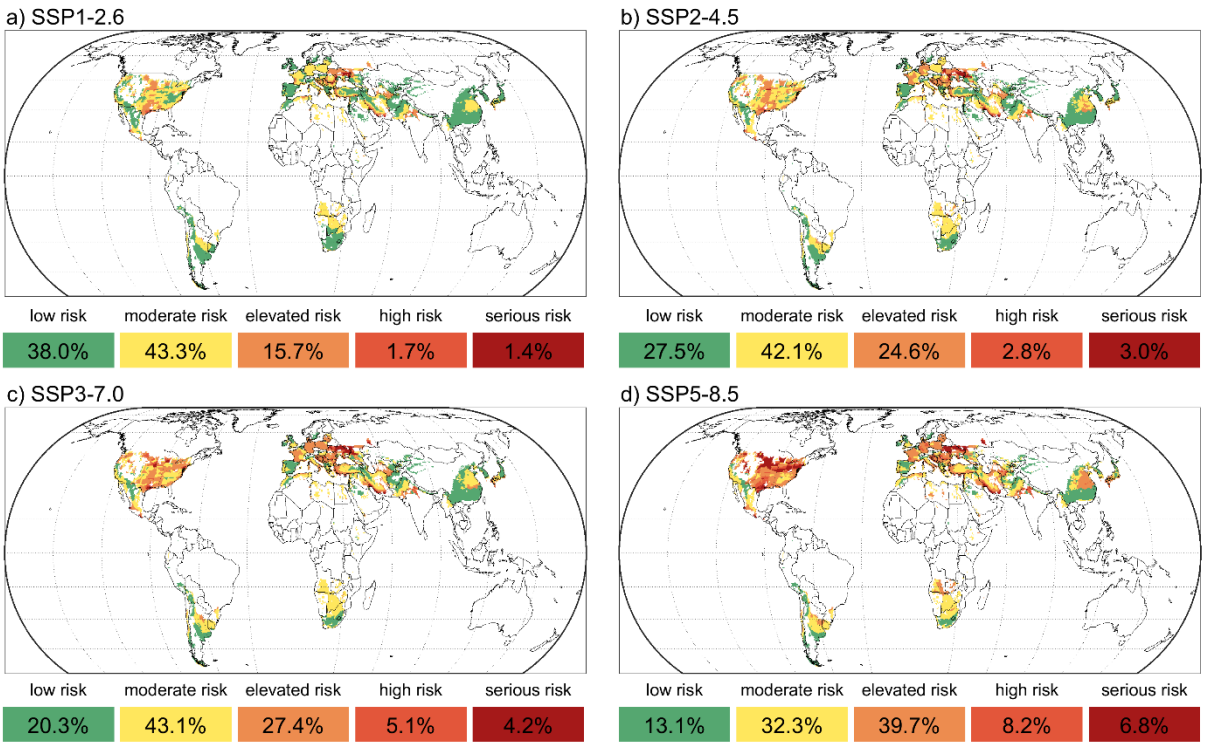

Figure S12: Same as Figure 4, but for winter wheat.

100

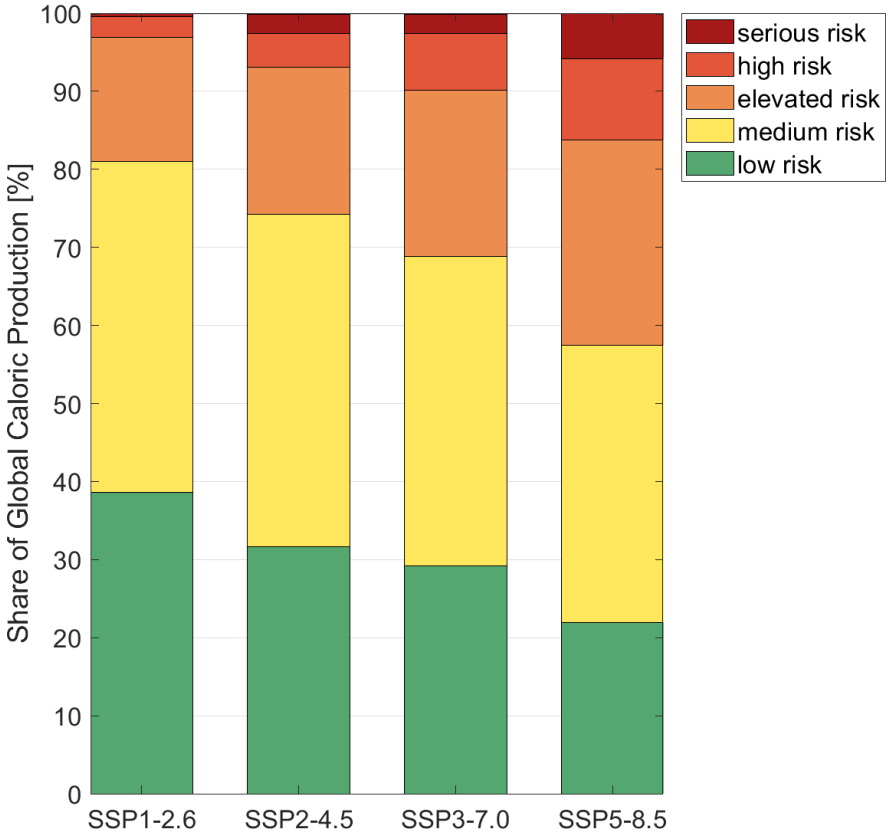

Figure S13: Same as Figure 5, but share of global caloric production on each of the different risk classes.

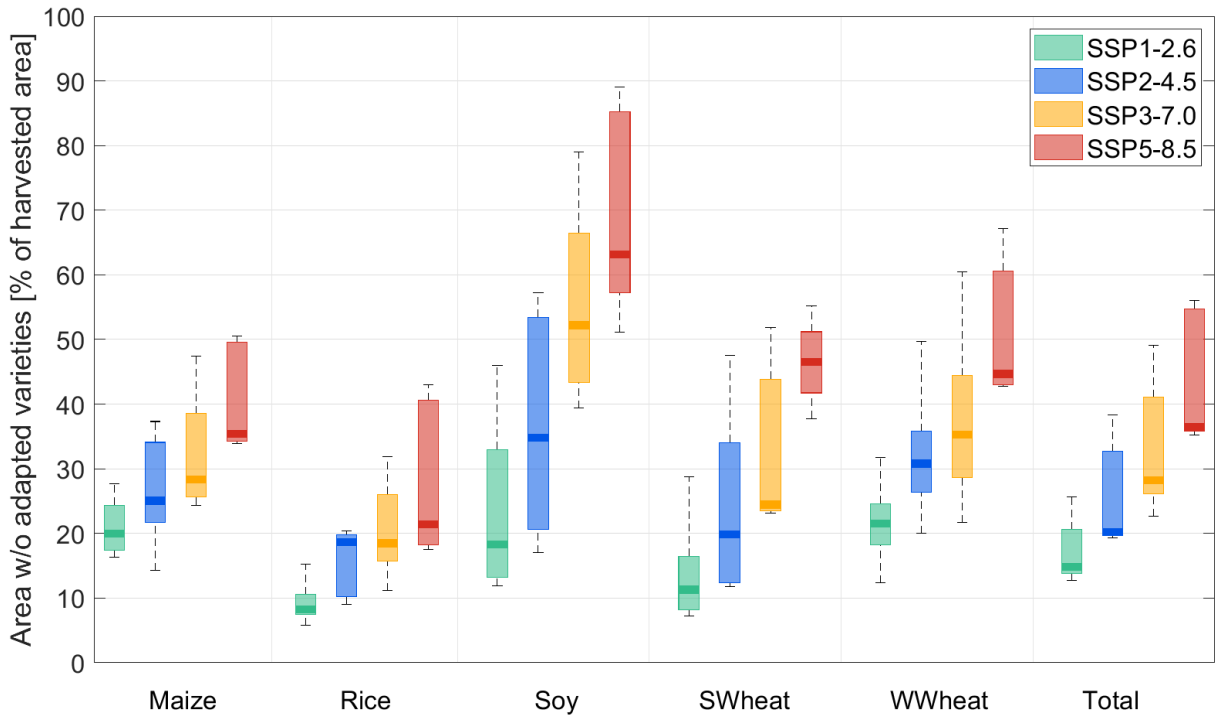

Figure S14: Percentage area without adapted varieties for different SSPs (2070-2100). Areas with elevated, high and serious risk for unavailable adapted varieties are considered and are shown in percent of total harvested area for SSP1-2.6 (green), SSP2-4.5 (blue), SSP3-7.0 (yellow) and SSP5-8.5 (red) for five crops (maize, rice, soy, spring wheat, winter wheat), and their cumulative total area. Boxplots show the range of five climate models.

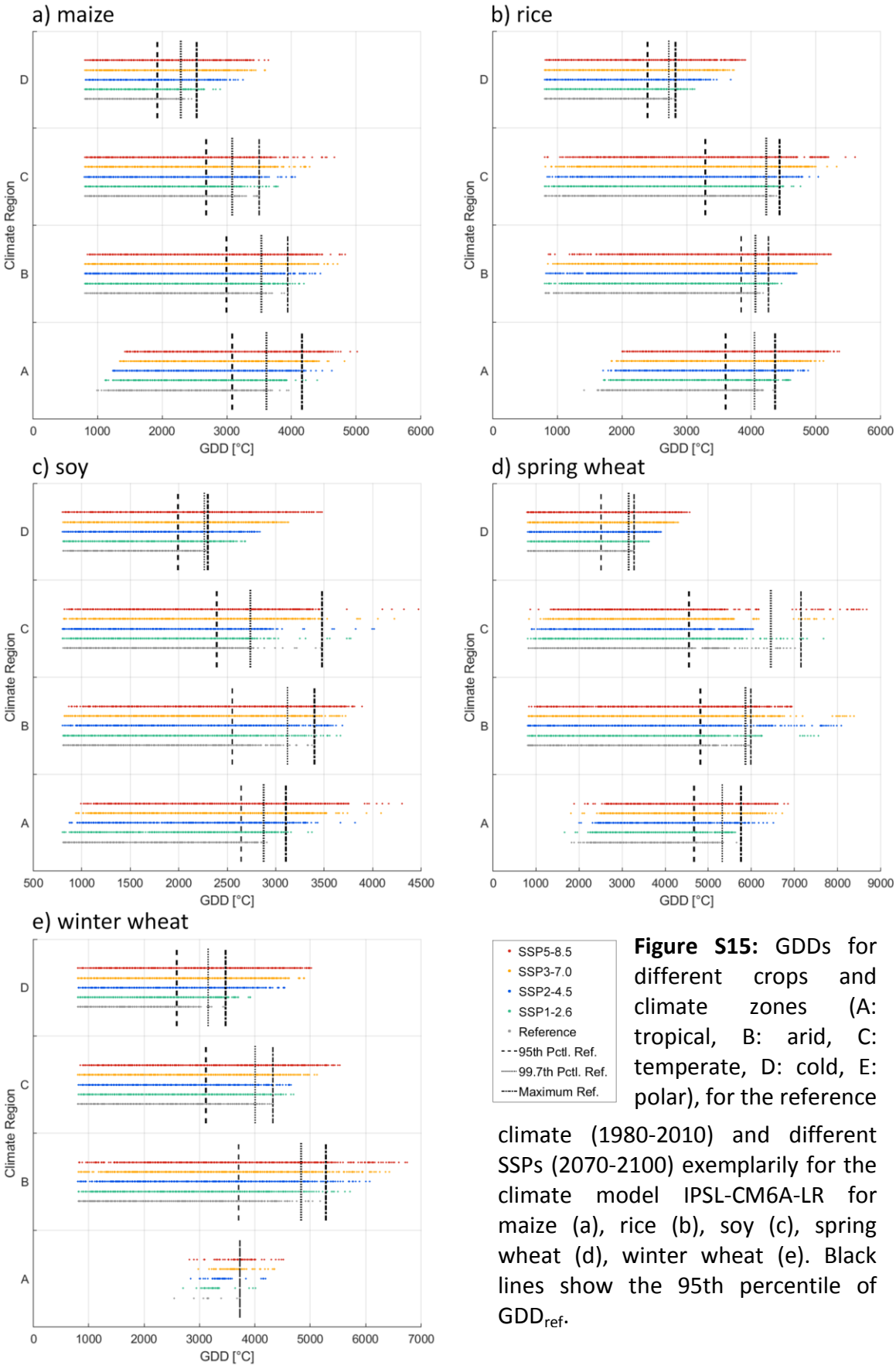

Figure S15: GDDs for different crops and climate zones (A: tropical, B: arid, C: temperate, D: cold, E: polar), for the reference climate (1980-2010) and different SSPs (2070-2100) exemplarily for the climate model IPSL-CM6A-LR for maize (a), rice (b), soy (c), spring wheat (d), winter wheat (e). Black lines show the 95th percentile of GDD_{ref}.

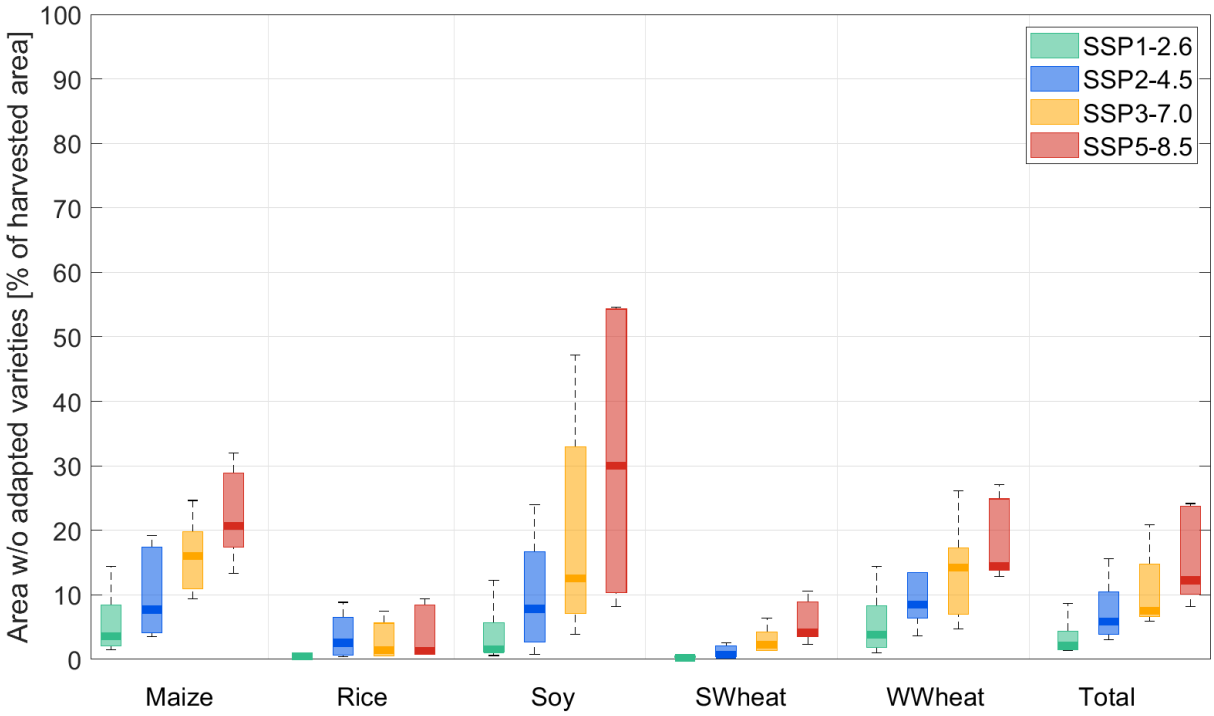

Figure S16: Same as Fig. S14, but for high and serious risk areas only.

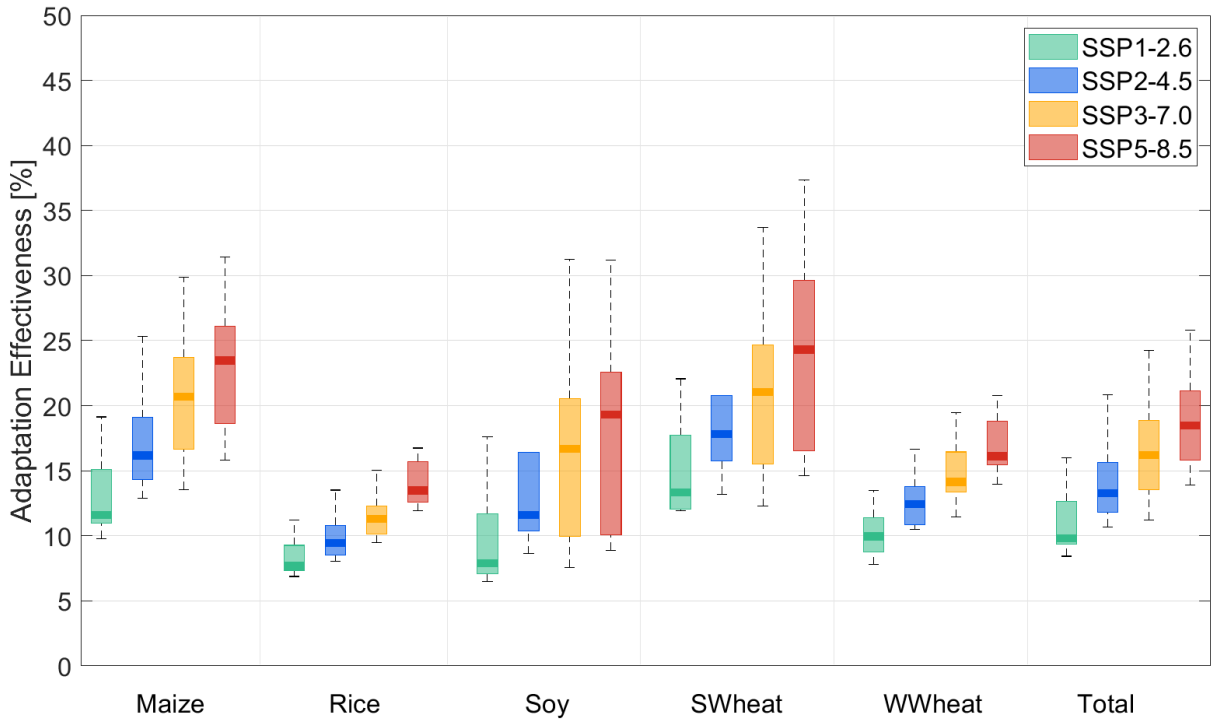

Figure S17: Same as Fig. 6, but range is only shown over climate models. Therefore, the median crop model has been combined with all climate models.

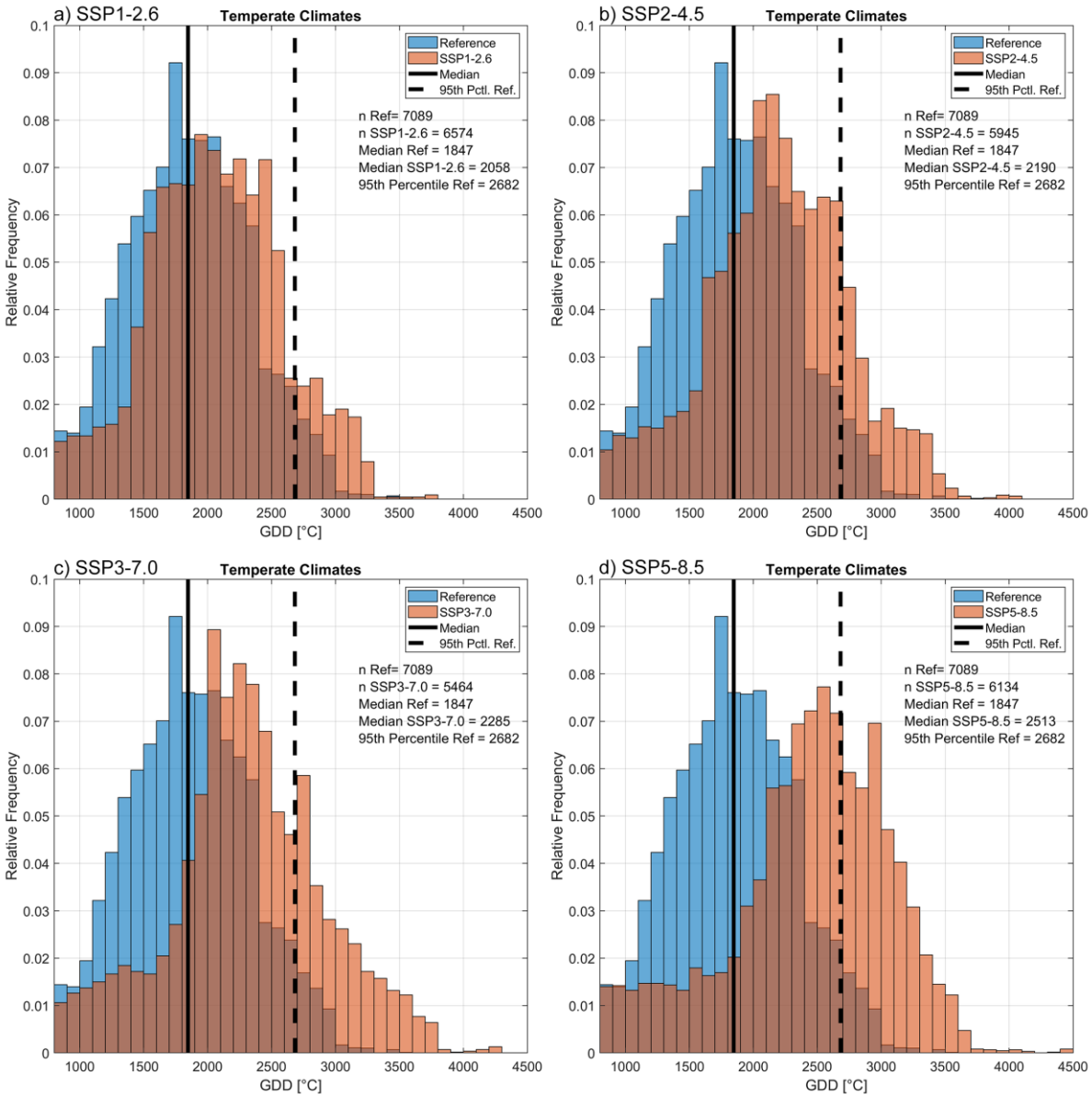

120

Figure S18: Same as Fig. S1, but exemplarily stratified for Koeppen-Geiger region C (temperate climate).

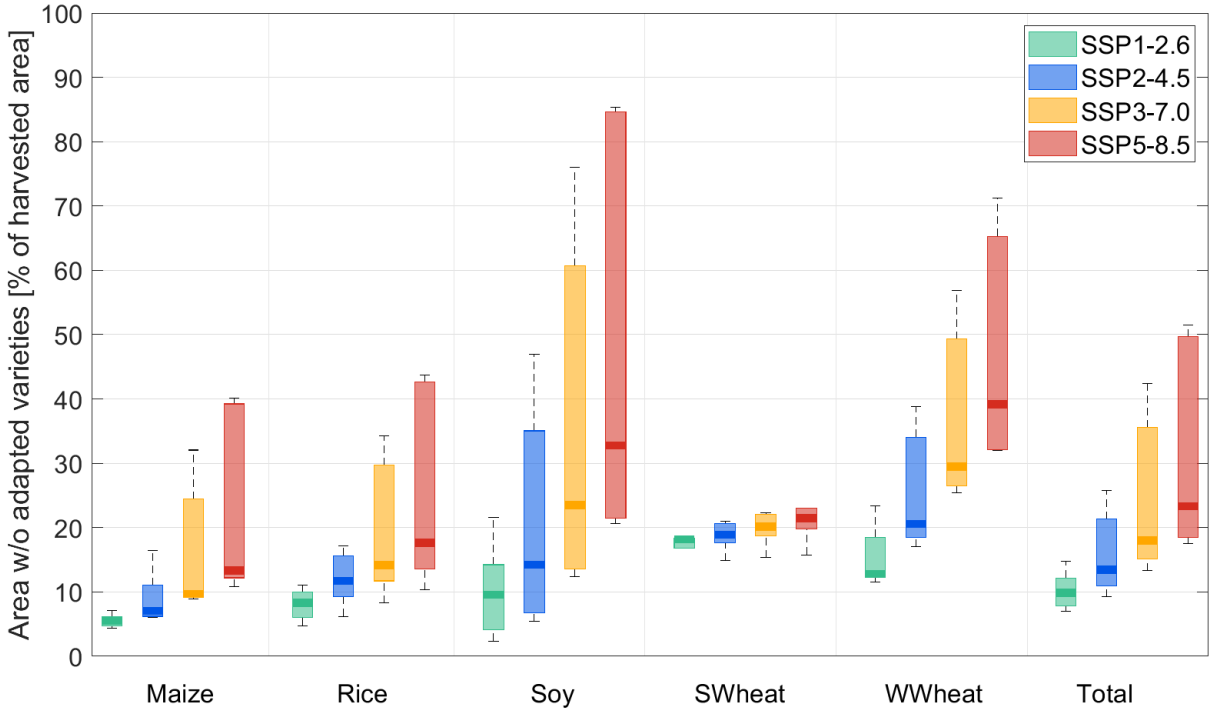

Figure S19: Same as Fig. S14, but without climate-zone stratification.

125

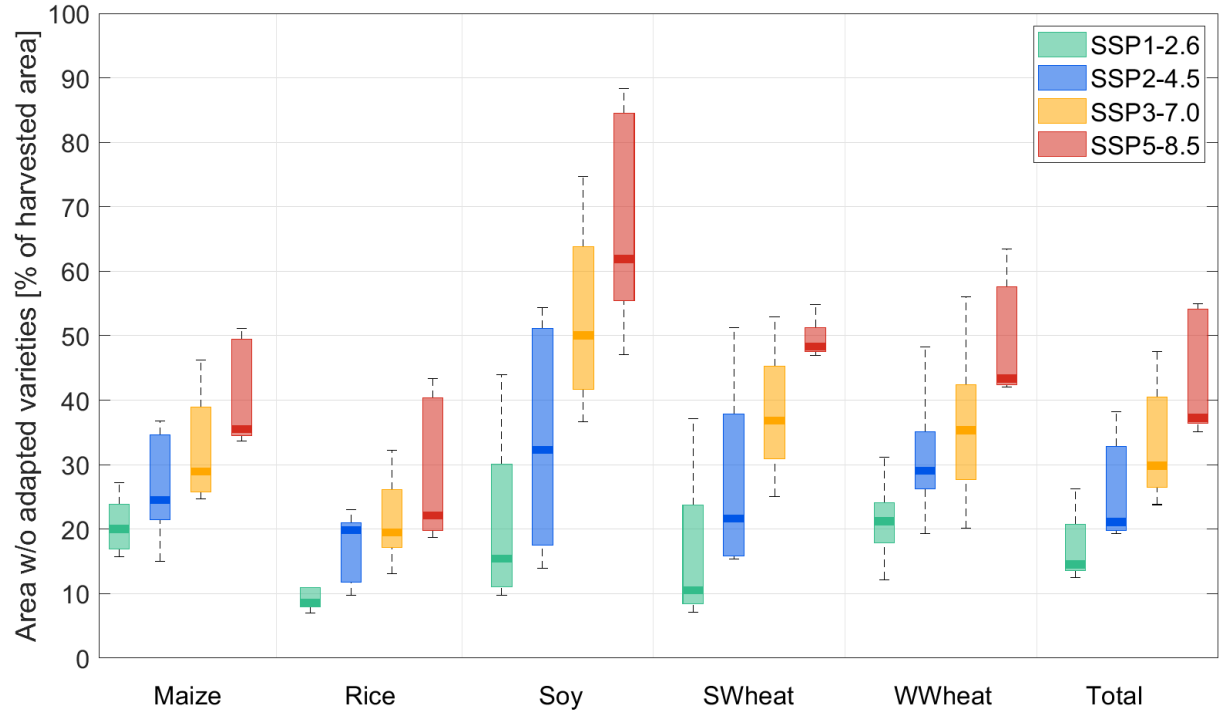

Figure S20: Same as Fig. S14, but excluding areas smaller than 10 ha per pixel.

Supplementary Note 1:

Climate zone stratification ignores that transitions between climate zones can be smooth. Consequently, patterns along climate zone boundaries could be too harsh in our results, since they pose hard thresholds of different climates, along which we assume no transferability between varieties. We tested the sensitivity to the Koeppen-Geiger stratification. Without restricting the transferability of varieties to same Koeppen-Geiger regions, the median of total area with unavailable adapted varieties globally decreases by 14 percentage points for SSP5-8.5 (Fig. S19). Rice and winter wheat are least affected by the climate zone stratification, since the global distribution is mainly concentrated within the tropical and temperate zone, respectively.

Supplementary Note 2:

An exclusion of crop areas below 10 ha (per pixel) was tested to evaluate the effect of rare varieties that are cultivated on only small areas. Figure S20 shows that although the areas account for only 0.011% of global harvested areas, total caloric production increased by 0.9 pp for SSP5-8.5 when we considered these varieties for adaptation. The example illustrates that small areas can be of disproportionate importance for genetic diversity, but have no relevant influence on the globally aggregated results. Nevertheless, the applied empirical analysis may underestimate the diversity of existing varieties, because natural or rare varieties that are not widely cultivated may not be captured by statistical records and are thus not considered in this study. However, these varieties could potentially hold valuable genetic information required for breeding more resilient varieties.